Intraarticular injection of relaxin-2 alleviates shoulder arthrofibrosis

William A. Blessing[a,b,c,1], Stephen M. Okajima[d,1], M. Belen Cubria[d,1], Juan C. Villa-Camacho[d], Miguel Perez-Viloria[d], Patrick M. Williamson[d], Angie N. Sabogal[d], Sebastian Suarez[d], Lay-Hong Ang[e], Suzanne White[e], Evelyn Flynn[f], Edward K. Rodriguez[d,2,3], Mark W. Grinstaff[a,b,c,2,3], and Ara Nazarian[d,g,2,3]

[a]Department of Biomedical Engineering, Boston University, Boston, MA 02215; [b]Department of Chemistry, Boston University, Boston, MA 02215; [c]Department of Medicine, Boston University, Boston, MA 02215; [d]Center for Advanced Orthopaedic Studies, Beth Israel Deaconess Medical Center, Harvard Medical School, Boston, MA 02115; [e]Confocal Imaging and IHC Core, Beth Israel Deaconess Medical Center, Harvard Medical School, Boston, MA 02115; [f]Orthopedic Research Laboratories, Boston Children's Hospital, Harvard Medical School, Boston, MA 02115; and [g]Department of Orthopaedic Surgery, Yerevan State Medical University, Yerevan 0025, Armenia

Edited by Robert Langer, Massachusetts Institute of Technology, Cambridge, MA, and approved May 9, 2019 (received for review January 10, 2019)

Arthrofibrosis is a prevalent condition affecting greater than 5% of the general population and leads to a painful decrease in joint range of motion (ROM) and loss of independence due to pathologic accumulation of periarticular scar tissue. Current treatment options are limited in effectiveness and do not address the underlying cause of the condition: accumulation of fibrotic collagenous tissue. Herein, the naturally occurring peptide hormone relaxin-2 is administered for the treatment of adhesive capsulitis (frozen shoulder) and to restore glenohumeral ROM in shoulder arthrofibrosis. Recombinant human relaxin-2 down-regulates type I collagen and α smooth muscle actin production and increases intracellular cAMP concentration in human fibroblast-like synoviocytes, consistent with a mechanism of extracellular matrix degradation and remodeling. Pharmacokinetic profiling of a bolus administration into the glenohumeral joint space reveals the brief systemic and intraarticular (IA) half-lives of relaxin-2: 0.96 h and 0.62 h, respectively. Furthermore, using an established, immobilization murine model of shoulder arthrofibrosis, multiple IA injections of human relaxin-2 significantly improve ROM, returning it to baseline measurements collected before limb immobilization. This is in contrast to single IA (sIA) or multiple i.v. (mIV) injections of relaxin-2 with which the ROM remains constrained. The histological hallmarks of contracture (e.g., fibrotic adhesions and reduced joint space) are absent in the animals treated with multiple IA injections of relaxin-2 compared with the untreated control and the sIA- and mIV-treated animals. As these findings show, local delivery of relaxin-2 is an innovative treatment of shoulder arthrofibrosis.

relaxin | fibrosis | frozen shoulder | arthrofibrosis

Arthrofibrosis is an accumulation of fibrotic collagenous tissue within the joint, frequently occurring after trauma, surgical procedures, inflammation, prolonged joint immobilization, or idiopathically (1–5). It manifests as a painful and longstanding restriction of joint range of motion (ROM) (6). Depending on severity and joint location, patients experience limitations in performing even basic activities of daily living, such as ambulation, self-care, and ability to work, thus significantly undermining quality of life for prolonged periods of a year or more (7).

Most limiting in the shoulder, knee, hip, wrist, and ankle, the incidences of arthrofibrosis are remarkably high. In the United States alone, close to 3 million individuals are subjected to procedures attempting to alleviate arthrofibrosis every year (Table 1) (8–20). For instance, the incidence of knee arthrofibrosis cases that require surgical intervention is 14.5% after intraarticular (IA) fractures or other trauma (21). The prevalence of arthrofibrosis following anterior cruciate ligament reconstruction is as high as 35%. The frequency of arthrofibrosis in the shoulder is up to 5% of the general population, increasing to 36% among those suffering from diabetes (5, 22–25).

Current treatment options for patients suffering from arthrofibrosis are limited in scope and effectiveness. Nonsurgical treatments, such as physical therapy, IA corticosteroid injections, NSAIDs, and nerve blockers provide only marginal or temporary relief of symptoms (5, 26). Current drug treatments target COX-1, COX-2, and glucocorticoid receptors to reduce symptoms without addressing the source of inflammation or the accumulation of fibrotic collagenous tissue. In more severe cases of the disease, surgical interventions such as physical manipulation of an affected joint under anesthesia and capsulotomies may improve ROM and alleviate pain but at the risk of further aggravating the condition (5) or sustaining other complications.

As an alternative to current arthrofibrosis treatments, we propose the local delivery of recombinant human relaxin-2 to address the underlying cause of the condition: accumulation of fibrotic, collagenous tissue. Relaxin-2 is a native antifibrotic hormone upregulated during pregnancy to increase tissue laxity by promoting matrix metalloproteinase (MMP) production and by repressing collagen production and expression of tissue inhibitors of metalloproteinases (TIMPs) and TGF-β1 (27–29). The use of relaxin-2 has been previously studied in other fibrotic disease present in

Significance

The accumulation of fibrotic collagenous tissue within the shoulder, knee, and elbow synovial joints restricts movement and causes pain. Current treatments for such arthrofibroses focus on pain management (corticosteroids) and do not reduce or eliminate the fibrotic tissue buildup in the joint. We report the natural protein hormone relaxin-2 as a treatment for shoulder arthrofibrosis (i.e., frozen shoulder). Multiple intraarticular injections of human relaxin-2 restore range of motion and eliminate capsular fibrosis in a murine model of shoulder arthrofibrosis. Encouraging results from both cell and animal studies support further development and clinical evaluation of relaxin-2 as a first-in-kind therapy for arthrofibroses.

Author contributions: W.A.B., S.M.O., M.B.C., J.C.V.-C., E.K.R., M.W.G., and A.N. designed research; W.A.B., S.M.O., M.B.C., J.C.V.-C., M.P.-V., P.M.W., A.N.S., S.S., L.-H.A., S.W., E.F., E.K.R., M.W.G., and A.N. performed research; W.A.B., J.C.V.-C., M.P.-V., and P.M.W. contributed new reagents/analytic tools; W.A.B., S.M.O., J.C.V.-C., S.W., E.K.R., M.W.G., and A.N. analyzed data; and W.A.B., S.M.O., E.K.R., M.W.G., and A.N. wrote the paper.

Conflict of interest statement: M.W.G., E.K.R., and A.N. are coinventors on a patent application submitted to the United States Patent and Trademark Office on the application of human relxin-2 as a treatment for arthrofibrosis.

This article is a PNAS Direct Submission.

Data deposition: Pharmacokinetic data related to this paper have been provided in Dataset S1.

[1]W.A.B., S.M.O., and M.B.C. contributed equally to this work.

[2]E.K.R., M.W.G., and A.N. contributed equally to this work.

[3]To whom correspondence may be addressed. Email: ekrodrig@bidmc.harvard.edu, mgrin@bu.edu, or anazaria@bidmc.harvard.edu.

This article contains supporting information online at www.pnas.org/lookup/suppl/doi:10.1073/pnas.1900355116/-/DCSupplemental.

Published online June 3, 2019.

Table 1. Frequency of arthrofibrosis events requiring further care in select upper and lower extremity joint cases in the United States per year

Case	No. of procedures	No. (%) of patients treated with interventional or preventative care	
		Surgical	Nonsurgical
Lower extremity			
Total knee arthroplasty	700,000[8]	42,000 (6)[9]	658,000 (94)[10]
Anterior cruciate ligament repair	222,950[11]	4,459 (2)[12]	218,491 (98)[13]
Meniscus repair	500,000[14]	5,000 (1)*	495,000 (99)[15]
Knee trauma	318,663[16]	15,933 (5)	302,730 (95)[5]
Upper extremity			
Elbow trauma	48,000[17]	672 (1.4)[17]	47,328 (98.6)[17]
Shoulder trauma	370,000[18]	3,700 (1)*	366,300 (99)†
Frozen shoulder	1,625,000[1]	162,500 (10)	1,462,500 (90)†
Distal radius fracture	300,000[19]	3,000 (1)*	297,000 (99)†
Total shoulder replacement	53,000[20]	530 (1)*	52,470 (99)†
Total	4,137,613	237,794	3,899,819

*Surgical intervention to address arthrofibrosis is rare for these cases.
†Occurrence of arthrofibrosis is all but certain for these conditions.

the heart, lungs, kidney, and liver (30–35). Our proposal stems from anecdotal clinical observation among a cohort of arthrofibrosis-afflicted female patients who experienced lasting motion restoration and reduced joint pain during and after pregnancy (E.K.R.). Consistent with this observation, data collected on pregnant animal models showed a reduction in joint stiffness, reduced collagen content, and fewer fibrocartilagenous cells in the joint, in addition to an increase in MMPs from up-regulated relaxin expression (27, 36, 37). Given that capsular fibrosis, rather than myogenic restriction, is primarily responsible for long-term ROM loss in arthrofibrosis (38), we hypothesize that relaxin-2 will reduce fibrosis in an immobilization shoulder joint contracture model, and as such its local administration will alleviate the symptoms and causes of arthrofibrosis. Herein, we report the activity of relaxin-2 to down-regulate collagen I expression in primary cultured human fibroblast-like synoviocytes (HFLS), the pharmacokinetic profiling and short in vivo half-life of relaxin-2 after IA injection into the glenohumeral joint, and the performance of relaxin-2 in an established murine model of shoulder arthrofibrosis (aka frozen shoulder). Multiple IA injections (mIA) of relaxin-2 into the glenohumeral joint, unlike multiple i.v. injections (mIV) or single IA injection (sIA), restore ROM and reduce fibrotic collagenous tissue compared with the untreated control animals.

Results

Human Relaxin-2 Effect on Collagen I Expression. In primary HFLS, basal levels of type I collagen expression in the presence of TGF-β1 were assessed by Western blotting in the presence and absence of relaxin-2. Cells treated with 10 and 50 ng/mL relaxin-2 did not show a difference in type I collagen expression compared with the untreated control, but treatment with relaxin-2 at 100 ng/mL resulted in a significant decrease in type I collagen, all relative to the expression of the housekeeping gene GAPDH (Fig. 1*A*). The down-regulation of type I collagen at 100 ng/mL was further validated with a quantitative cAMP assay (Fig. 1*B*). Previous studies showed that relaxin-2 binding to its receptor leads to G protein-coupled receptor signaling and hence an accumulation of cAMP (39). A 20-min stimulation of primary human synoviocytes with relaxin-2 affords an increase in intracellular cAMP levels at 100 ng/mL of relaxin-2 ($P < 0.01$). Lower concentrations did not induce a statistically significant increase in intracellular cAMP. Finally, treatment of human synoviocytes with TGF-β1 results in myofibroblast differentiation as noted by the up-regulation of α-smooth muscle actin (αSMA) (Fig. 1 *C*, *II*) compared with the untreated control (Fig. 1 C, *I*). The presence of relaxin-2 at a concentration of 100 ng/mL prevents myofibroblast differentiation in the presence of TGFβ1 (Fig. 1 C, *III*).

Pharmacokinetic Profiling of IA Administration of Relaxin-2. To determine the pharmacokinetic profile of relaxin-2 after IA injection, we locally administrated 10 μg/kg of relaxin-2 directly into the glenohumeral joint of healthy Sprague-Dawley rats (Table 2). The resulting relaxin-2 concentrations in the serum, synovium, and organs were analyzed using compartmental analysis. A two-compartmental model provided the best goodness of fit for the synovial joint space and other organs, and a single compartmental model provided the best goodness of fit for serum relaxin-2 (Table 2 and *SI Appendix*, Fig. S2 and Table S1). All of the pharmacokinetic parameters are listed in Table 2, but

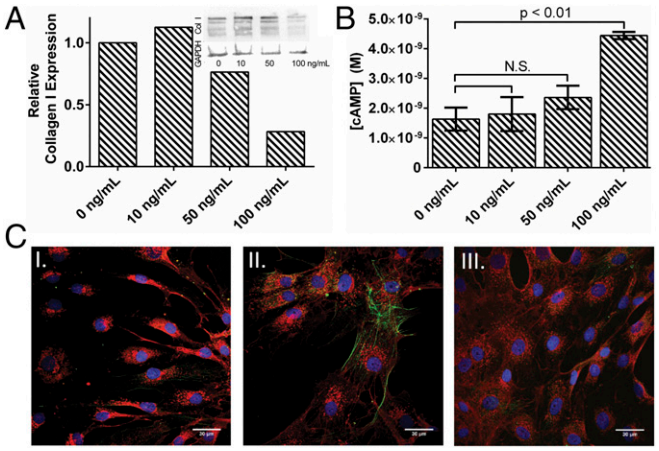

Fig. 1. In vitro biochemical investigation of relaxin-2 in synoviocytes. (*A*) Western blot (*Inset*) analysis reveals that collagen I expression decreases to 25% with 100 ng/mL of relaxin-2 in the presence of TGF-β relative to a GAPDH loading control. (*B*) Relaxin-2 treatment stimulates cAMP production at 100 ng/mL, consistent with the down-regulation in collagen I. (*C*) Human synoviocytes treated with relaxin show a decrease in myofibroblast differentiation. (*I*) Untreated synoviocytes (red, membrane; blue, nucleus) show minimal expression of αSMA (green). (*II*) Synoviocytes treated with 5 ng/mL TGFβ1 show increased myofibroblast differentiation as denoted by increased αSMA expression. (*III*) Treatment with 100 ng/mL relaxin-2 precludes myofibroblast differentiation in the presence of TGFβ1.

of note, the elimination and distribution half-lives in the synovium were determined to be 0.618 (95% CI: 0.49, 0.65) and 4.61 (1.8, 5.1) h, respectively. In serum, the half-life was found to be 0.957 (0.75, 1.1) h. The mean residence time in each tissue was calculated to be 0.919 (0.79, 0.97) and 1.38 (1.1, 1.6) h in the synovium and serum, respectively.

The pharmacokinetic results were validated with immuno- and histochemical analyses (Fig. 2). Relaxin-2 accumulates in the tissues surrounding the joint capsule and the humeral head within the synovial joint space (Fig. 2, *Left*). Anti-relaxin staining (Fig. 2, *Left*) shows the presence of relaxin at all time points. Intracellular inclusions of relaxin-2 are evident in the chondrocytes from the superficial layer of the articular cartilage. There is a rapid decrease of relaxin-2 staining over the course of 24 h. In this same time frame, the architecture (Fig. 2, *Middle*) and the integrity of the joint surface (Fig. 2, *Right*) are largely unchanged and show healthy cellular organization and cartilage content respectively. The distribution of relaxin-2 in the heart, liver, kidneys, and spleen was also investigated via immunohistochemistry (*SI Appendix*, Fig. S3). Briefly, in the heart, anti-relaxin staining was more predominant in the left ventricle, with an eccentric distribution pattern. In the kidneys, relaxin-2 accumulation appears to be more densely associated with the renal cortex at the early time points, and it begins to shift toward the hilum or the organ at the later time points. Relaxin-2 is present inside the tubule-glomerular cells of the nephrons. In the liver, relaxin-2 is organized intracellularly in the hepatic parenchyma without prominent distribution in any anatomical regions of the organ. The spleen shows an accentuated staining intensity within the red pulp. All organs show an initial heavy presence of relaxin-2 within the first 3 and 12 h, which decreases after 24 h. Lingering staining in all organs agrees with the longer distribution half-lives of each organ: these data are consistent with the pharmacokinetic modeling of these organs (*SI Appendix*, Table S1). H&E histochemical staining was also performed in all aforementioned organs (*SI Appendix*, Fig. S4), exhibiting no distinct morphological changes in any of the tissues over the course of 48 h after relaxin-2 injection. In summary, relaxin-2 treatment results in no aberrant morphological or tissue changes in the synovial space, the articular cartilage, or in the peripheral organs.

Relaxin-2 Activity in an in Vivo Shoulder Arthrofibrosis Model. To test our hypothesis, we evaluated the efficacy of human relaxin-2 to treat established shoulder arthrofibrosis. We performed an in vivo experiment using a rat model ($n = 20$) where shoulder arthrofibrosis was produced via an immobilization procedure (40). In this model, fibrosis is induced after 8 wk of forelimb immobilization by suturing the humeral shaft to the scapula, as measured by histochemical and biomechanical analyses (*SI Appendix*, Figs. S5 and S6). At a healthy baseline before forelimb immobilization, all rats attained a full ROM, with the total ROM, defined as the sum of the internal and external ROM, of 159.17° ± 0.94°. After surgical induction of shoulder joint contracture followed by 8 wk of immobilization and subsequent suture removal, a significant reduction in total ROM of the forelimb was observed in all animals (91.17° ± 10.11°, 43.22 ± 6.31%; Fig. 3*A*) compared with healthy baseline ($P < 0.01$).

After forelimb immobilization and formation of arthrofibrosis, the animals were randomly selected to receive relaxin-2 by a single IA injection at 6 μg/kg, multiple IA doses of relaxin-2 every 2 d for 10 d (five relaxin-2 doses of 2 μg/kg for a total dose of 10 μg/kg), or multiple i.v. tail vain injections every 2 d for 10 d (five relaxin-2 doses of 680 μg/kg for a total dose of 3.4 mg/kg). No differences in ROM were observed between the untreated control group and all treatment groups at the beginning of the experiment, that is, immediately after suture removal [mIA ($P = 0.48$), sIA ($P = 0.93$), and mIV ($P = 0.99$)]. The animals did not exhibit any adverse events or modified behavior toward either relaxin-2 injection or biomechanical measurements. This observation is consistent with the lack of toxicity observed in previous studies, which administered a single dose of up to 463 μg/kg (41, 42).

The ROM measurements over the subsequent 8 wk are presented in Table 3 and Fig. 3. The total ROM of untreated control group remained constricted by −24.0°, or −14.8% ($P < 0.01$) for the duration of the experiment compared with healthy baseline, a finding consistent with previous studies (42, 43). Similarly, the mIV treatment group displayed a significant restriction of −31.0°, or −19.3% ($P < 0.01$) in total ROM over the 8 wk compared with healthy baseline. For the sIA treatment group, in comparison with the untreated controls, there was a temporary improvement in the total ROM measurement directly following the treatment ($P = 0.025$). However, the animals in the sIA group returned to a restricted total ROM by day 14 and remained restricted by −21.0°, or −13.5% ($P < 0.01$) for the duration of the experiment. The results from the mIA treatment group were significantly improved compared with the untreated

Table 2. Pharmacokinetic profile of IA relaxin-2 (10 μg/kg) in the synovial joint space

Parameter	Synovium (low 95% CI, high 95% CI)	Serum (low 95% CI, high 95% CI)
k_{10}, h^{-1}	1.12 (1.3, 1.0)	0.724 (0.92, 0.63)
k_{12}, h^{-1}	0.00411 (3.6×10^{-2}, 3.0×10^{-3})	—
k_{21}, h^{-1}	0.151 (0.39, 0.13)	—
$t_{1/2\alpha}$, h	0.618 (0.49, 0.65)	0.957 (0.75, 1.1)
$t_{1/2\beta}$, h	4.61 (1.8, 5.1)	—
C_0, pg/mL	2.91×10^5 (2.0×10^5, 3.9×10^5)	1.84×10^5 (1.7×10^5, 2.1×10^5)
V, mL	8.56 (12, 6.4)	135 (140, 120)
CL, mL/h	9.57 (17, 6.7)	98.2 (130, 77)
V_2, mL	0.233 (1.1, 0.14)	—
CL_2, mL/h	0.0353 (0.45, 1.9×10^{-2})	—
AUC_{0-24h}, pg·h/mL	2.61×10^5 (1.5×10^5, 3.7×10^5)	2.54×10^5 (1.9×10^4, 3.2×10^4)
AUMC, pg·h^2/mL	2.40×10^5 (1.2×10^5, 3.6×10^5)	3.51×10^5 (2.0×10^4, 5.1×10^4)
MRT, h	0.919 (0.79, 0.97)	1.38 (1.1, 1.6)
V_{ss}, mL	8.80 (13, 6.6)	135 (140, 120)

k_{10}, k_{12}, k_{21}, rate constants associated with elimination (k_{10}) and flux between compartments (k_{12} and k_{21}); $t_{1/2\alpha}$, elimination half life of relaxin; $t_{1/2\beta}$, terminal half life of relaxin; C_0, intial relaxin concentration after administration; V_2, volume of distribution (per compartment); CL_2, clearance (per compartment); $AUC_{0\text{-}24h}$, area under the concentration vs. time curve from 0–24 h; AUMC, area under first moment curve; MRT, mean residence time; V_{ss}, volume of distribution at steady state.

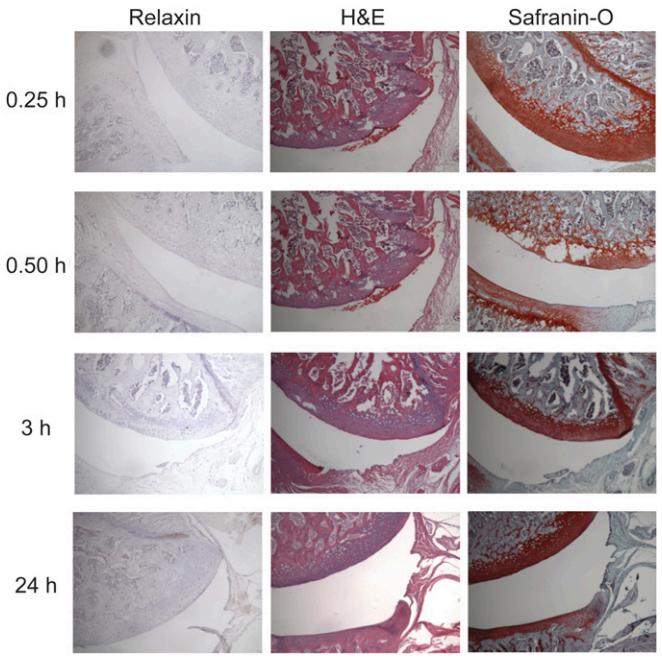

Fig. 2. Relaxin-2 does not change the healthy architecture of the synovial joint space. Over the course of 24 h, the integrity of the synovial joint space is maintained. (*Left*) Anti-relaxin-2 staining shows the accumulation of relaxin-2 around the periphery of the synovial joint space without infiltration into the humeral head. After 24 h (*Bottom Left*), relaxin-2 staining is minimal, indicating that it has been dispersed from the synovial joint. (*Middle*) The cellular organization and architecture of the relaxin-2 treatment remains healthy. There is no notable increase in cell death. (*Right*) Safranin-O staining shows that the integrity of the joint is maintained. After 24 h, the margins of GAG and cartilage content remain the same as indicated by the orange surface on the humeral head and the joint capsule.

control group ($P < 0.01$) and not statistically different from the healthy baseline measurements ($P = 0.94$).

Separate analyses of forelimb internal and external ROM measurements of the sIA and mIV treatment groups indicated no significant differences with the untreated control group (*P* values in Table 3). Also, no differences were observed in the external ROM among all treatment groups and the untreated control group at the final measurement (*P* values in Table 3 and Fig. 3*B*). Significant improvements in internal ROM were observed only in the mIA group ($P < 0.01$). Improvements in ROM in the mIA group occurred at the second measurement time point and continued until the final measurement (Fig. 3 *A* and *C*). The mIA and the healthy baseline groups exhibited identical torque per angle profiles, while the profiles of the sIA and mIV deviated from that of the healthy baseline (Fig. 3*D*). Restoration of full internal ROM for the mIA group was also observed, whereas other treatment groups showed similarly constricted internal ROM compared with the untreated control group (Fig. 3*C*). Fig. 3*B* highlights the similarity of external ROM across all groups. The healthy contralateral forelimbs showed no significant change from healthy baseline for the final ROM measurements across all groups except for mIV, which became more restricted at the final measurement (Table 4 and *SI Appendix*, Fig. S6). There was no indication of an increase in contralateral joint laxity across treatment groups. All data were normally distributed based on the Shapiro–Wilk test for normality ($P = 0.54$).

Histology. Histological comparison of the mIA group with the untreated group as well as the healthy untreated control group was performed to examine any morphological changes in the only group that displayed significant restorative biomechanical changes. The H&E-stained sections of the untreated control group showed morphological changes to the surrounding capsular tissue compared with the healthy baseline. In the healthy baseline joint, a well-delineated separation was observed between the capsule and the articular surface on the humeral head (Fig. 4 *A*, *I*). The synovial membrane and the articular cartilage showed normal cellular organization. However, the joint in the untreated control group lacked this separation in the most inferior aspect of the glenohumeral joint and showed evidence of capsular adhesions (Fig. 4 *A*, *II*, yellow arrow). The capsule tightly surrounded the humeral head and obliterated peripheral spaces around the joint cavity, characteristic of a contracture (44) (Fig. 4 *A*, *II*, green arrow). The membrane and cartilage nuclei failed to maintain the expected tangential orientation to the humeral head within the superficial zone (tangential zone), and some of the surrounding fibrotic cells showed an orthogonal directionality from the expected surface contour (Fig. 4 *A*, *II*, white box).

In contrast to the untreated control, the mIA group lacked any apparent adhesions (Fig. 4 *A*, *III*). The synovial membrane and the articular cartilage surfaces remained separated from one another. Analogous to the healthy baseline, proper cellular organization of these membranes was observed. However, in the mIA group, the amount of surrounding connective tissue was less observed compared with the tissue found in the healthy baseline. All histological sections in the mIA group also displayed fibrillation within the articular surface, which was not observed in the healthy baseline (Fig. 4 *A*, *III*, black arrows). These changes in articular cartilage quality in the mIA group were mild, akin to a grade 1 based on the Osteoarthritis Research Society International grading system (45, 46).

Sections stained for fibronectin showed an increase in fibrotic tissue and capsular tissue thickness in the untreated control group in comparison with the healthy baseline (Fig. 4 *B*, *I* and *II*, red bracket). Additionally, evidence of adipocyte infiltration was observed inferiorly within this tissue (Fig. 4 *B*, *II*, black arrows). These results are consistent with those reported by Kim et al. (47). The mIA group displayed a return to normal thickness in capsular tissue as well as a reduction in peroxidase intensity in and around the capsular tissue (Fig. 4 *B*, *III*, red bracket).

Discussion

Idiopathic, trauma-related, and postsurgical arthrofibroses affect millions of patients in the United States alone and tens of millions of individuals worldwide. Current pharmacological treatments are palliative and do not reduce or eliminate the fibrous tissue buildup within the joint. Surgery can remove some of the fibrotic burden; however, the surgical process itself further incites the inflammation cascade and results in rescarring of the joint capsule in addition to common potential procedural complications and limited long-term efficacy (48). Thus, there is a clinical need for alternative treatments that minimize IA disruption such as minimally invasive surgical procedures, or preferably, pharmacological interventions. Our search for a promising therapeutic modality for arthrofibrosis that addresses the underlying cause of the condition, accumulation of fibrotic collagenous tissue, led us to the reproductive hormone, relaxin-2.

Relaxin-2 is a 6-kDa peptide that induces growth and softening of the cervix, and is up-regulated naturally during child birth (25). Repurposing this peptide therapeutic for the treatment of arthrofibrosis provides an unprecedented opportunity to treat this disease with a first-in-kind therapy. Several studies report that relaxin-2 acts at multiple levels to inhibit fibrogenesis and collagen up-regulation associated with fibrosis and is able to prevent and treat pulmonary, renal, cardiac, and hepatic fibrosis in animal models (22, 24)—providing further motivation and a basis for this musculoskeletal application. In fact, relaxin-2 was assessed clinically for the treatment of heart failure, but the phase III clinical trial was halted due to limited efficacy after i.v. administration (42, 43). We propose that a localized injection into the synovial joint space may prolong its residence time at the

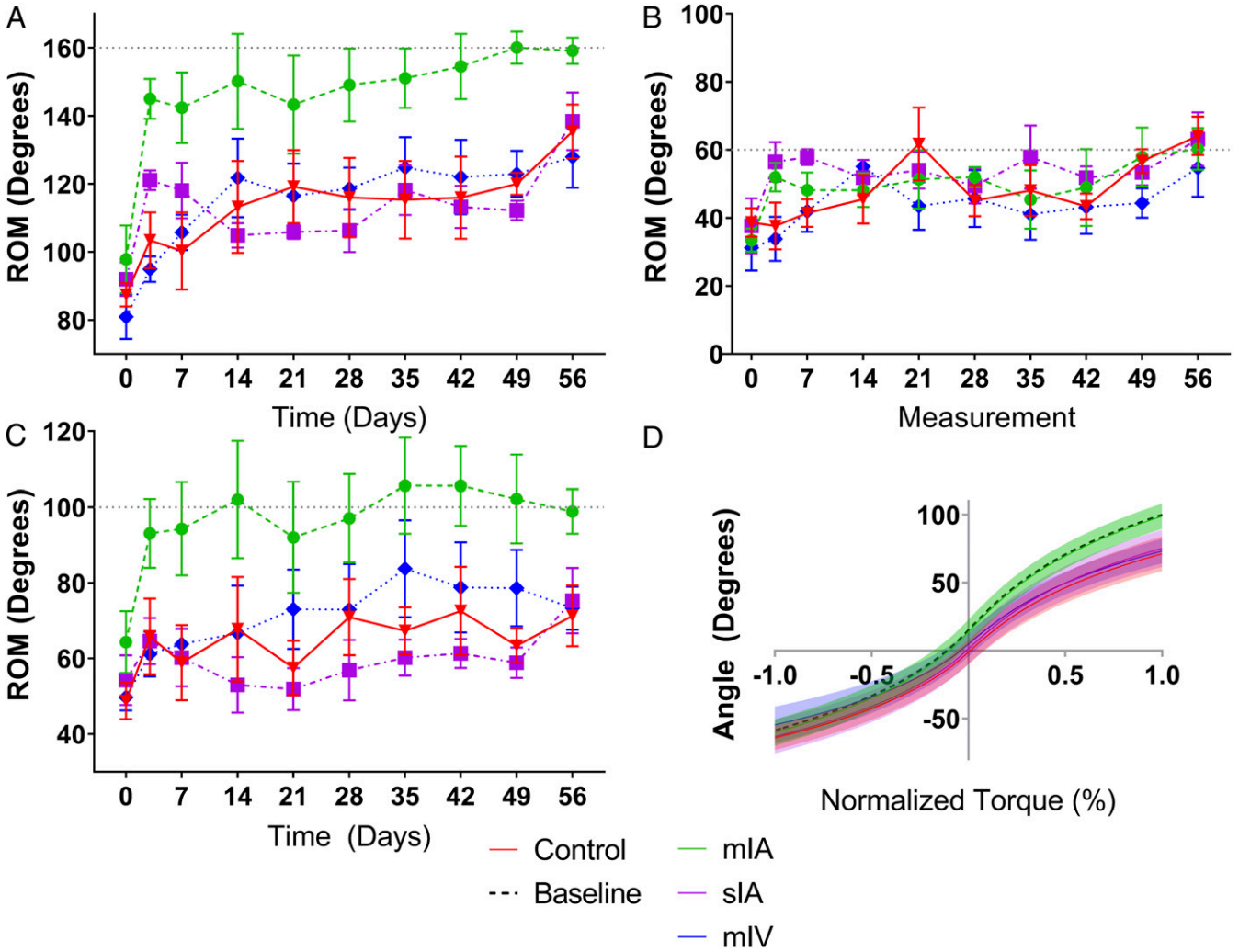

Fig. 3. mIA relaxin-2 induces a significant change in total ROM postsurgery. (*A*) Temporal results of the total ROM are presented as means with a 95% CI. Healthy baseline describes a healthy control, whereas untreated control describes the immobilized control group without any treatment. Day 0 signifies suture removal and the first measurement. Significance is defined at $\alpha = 0.05$. (*B*) Temporal results of external ROM. (*C*) Temporal results of internal ROM. (*D*) Normalized torque-angle curve of the final measurement; shaded colored regions signify a 95% CI. Negative angles and torques denote external rotation and positive angles denote internal rotation.

site and tissues of interest due to retention within the semipermeable synovial membrane and avascular anatomy of the articular surface of the joint. Here we describe the local IA administration of human relaxin-2 as a potential pharmacological treatment for frozen shoulder (i.e., shoulder arthrofibrosis).

Human relaxin-2 is expected to have biological, antifibrotic activity within the rat synovium due to its pleiotropic nature (49, 50), its structural homology to rat relaxin-1, and the presence of RXFP1 receptors in the rat shoulder joint and periphery (*SI Appendix*, Fig. S7) (47, 51). This human ortholog binds the rat RXFP1 more selectively and stimulates the antifibrotic cascade at a concentration two orders of magnitude less than its endogenous rat counterpart in vitro (52). Furthermore, relaxin-2's cross-species promiscuity and efficacy in previously reported in vivo rat (41), monkey (53), and human (54) tissues supports this conclusion (55).

Relaxin-2 up-regulates MMP production and fibronectin degradation and down-regulates collagen production and expression of TIMPs and TGF-β1 (27–29), leading to a net breakdown of extracellular matrix components (33, 56, 57). For example, relaxin-2 treatment of human fibroblasts causes a reduction in collagen types I and III and fibronectin. In cultured renal fibroblasts, epithelial cells, and mesangial cells, relaxin-2 decreases TGF-β1–induced fibronectin levels and increases fibronectin degradation (38). In vivo, relaxin-2 reduces bleomycin-induced collagen deposition in the lung and restores tissue to a healthy state (37). Finally, in pregnant animal models, relaxin-2 expression alters cartilage stiffness by activating MMP-1 and MMP-3, reducing collagen content and expression of fibrocartilagenous cells. Our results with HFLS, a major cellular component of the synovial joint, are consistent with these prior findings. In an in vitro setting, collagen expression decreases upon relaxin-2 treatment in the presence of TGF-β1 (Fig. 1*A*). Previous studies have shown that relaxin-2 binding to its G-coupled protein receptor (GPCR), RXFP1, inhibits TGF-β1 signaling and subsequently down-regulates collagen expression (58, 59). This GPCR activation is observed with relaxin-2 stimulation through production of cAMP (Fig. 1*B*). Furthermore, we show that relaxin-2 treatment prevents synovial fibroblast differentiation into myofibroblasts (Fig. 1*C*), as demonstrated by the lack of expressed αSMA fibers. Myofibroblasts are a major contributor to the fibrotic burden of the arthrofibrotic joint (60–62).

The role of relaxin-2 as a hormone to prime the pubic symphysis during pregnancy occurs with an increase in serum concentration before birth, followed by a rapid decrease postpartum (63–66). Several pharmacokinetic profiling studies of recombinant human relaxin-2 in humans, monkeys, and rats reveal its short elimination half-life [$t_{1/2}$ = 7 to 11 h (54), 3 to 7 min (53),

Table 3. Comparison of immobilized joint ranges of motion for each treatment group

Group	Baseline ROM, °	Final ROM, °	Difference				
			ROM (%Δ°)	95% CI (Δ°)		*F*	*P*
Total ROM							
Untreated	159 ± 1.3	135 ± 14	−14.8	−32.5	−16.7	116	—
mIA	158 ± 1.0	159 ± 6	0.21	−4.70	3.00		<0.01*
sIA	160 ± 0.90	138 ± 15	−13.5	−30.1	−13.1		0.99
mIV	158 ± 1.2	127 ± 16	−19.3	−41.1	−23.0		0.92
External ROM							
Untreated	59.3 ± 0.97	64.1 ± 10	8.09	−1.52	9.79		—
mIA	59.6 ± 0.58	60.2 ± 11	1.01	−5.86	6.39		0.99
sIA	60.0 ± 0.71	63.1 ± 14	5.22	−4.73	11.0		0.99
mIV	59.3 ± 0.85	54.6 ± 15	−7.87	−13.8	3.14		0.71
Internal ROM							
Untreated	99.7 ± 0.72	71.2 ± 14	−28.5	−36.8	−20.6		—
mIA	99.1 ± 0.61	98.8 ± 10	−0.27	−7.02	4.80		<0.01*
sIA	100 ± 0.69	75.2 ± 15	−24.8	−33.3	−16.0		0.99
mIV	99.3 ± 0.53	73.2 ± 10	−26.2	−32.4	−21.0		0.99

A complete ROM is expected to be near 160°. A negative change in ROM describes a difference in final ROM that is lower than a normal ROM. A positive change indicates a final ROM that is greater than the baseline measurement. Significance is determined at $\alpha = 0.05$. The *P* value is the result of a comparison between the untreated control ROM and the ROM of each of the different treatment groups.*Significance at $P < 0.05$.

and 1 to 2 min (41), respectively] after bolus i.v. injection. As the half-life after IA injection and the residence time in the glenohumeral joint are unknown and both are important for this particular application, we performed a pharmacokinetic study in rats. We hypothesize that when administered directly into the synovial joint space, relaxin-2 will exhibit an increased residence time due to the semipermeable nature of the synovial membrane and the avascular nature of the articular surface. The elimination half-life of relaxin-2 in the synovium is 0.61 (95% CI: 0.49, 0.65) h with a terminal half-life of 4.61 (1.8, 5.1) h, while the elimination half-life of relaxin-2 in the serum is 0.957 (0.75, 1.1) h. This serum half-life is not significantly longer than previously reported i.v. half-lives and is most likely influenced by the elimination and distribution from the synovial joint space. Furthermore, previous studies modeled the pharmacokinetics of systemic relaxin-2 via a noncompartmental analysis, whereas this study is based on a two-compartmental model that separately accounts for accumulation of relaxin-2 in each tissue. Notably, the IA administration allows the relaxin-2 to remain in high concentration in the synovium. For instance, the synovial concentration at 15 min after administration is 220 ng/mL and decreases to 120 ng/mL and then 1.83 ng/mL after 0.6 and 4.6 h, respectively (Table 2, *SI Appendix*, Fig. S2 and Table S1, and Dataset S1). The concentration in the serum after one half-life is 9.16 ng/mL and greater than baseline serum levels of <2 ng/mL (67). During rat pregnancy, relaxin is up-regulated to concentrations of 50 to 100 ng/mL in the serum (68). The elevated relaxin-2 concentration in the synovium after IA injection bodes well for performance in an efficacy study and suggests that multiple IA injections will perform superior to a single IA injection.

Table 4. Contralateral joint ranges of motion for each group to examine potential joint laxity

Group	Baseline ROM, °	Final ROM, °	Difference				
			ROM (%Δ°)	95% CI (Δ°)		*F*	*P*
Total ROM							
Untreated	159 ± 1.3	151 ± 7.2	−4.98	−18.8	2.90	158	—
mIA	158 ± 1.0	156 ± 11	−0.75	−12.0	9.67		0.99
sIA	160 ± 0.9	148 ± 6.4	−5.81	−20.8	2.26		0.99
mIV	158 ± 1.2	137 ± 11	−13.0	−31.2	−10.4		0.70
External ROM							
Untreated	59.3 ± 0.9	49.2 ± 14	−6.56	−21.3	0.38		—
mIA	59.6 ± 0.5	62.4 ± 11	2.26	−7.25	14.4		0.99
sIA	60.0 ± 0.7	37.0 ± 12	−14.1	−34.1	−11.0		0.99
mIV	59.3 ± 0.8	51.6 ± 15	−4.70	−17.9	2.85		0.99
Internal ROM							
Untreated	99.7 ± 0.7	102 ± 15	1.58	−8.35	13.3		—
mIA	99.1 ± 0.6	94.3 ± 14	−3.01	−15.6	6.05		0.99
sIA	100.1 ± 0.6	111 ± 14	8.34	1.79	24.8		0.99
mIV	99.3 ± 0.5	86.0 ± 8.0	−8.31	−23.6	−2.93		0.18

A complete ROM is expected to be near 160°. A negative change in ROM describes a difference in final ROM that is lower than a normal ROM. A positive change indicates a final ROM that is greater than the baseline measurement. Significance is determined at $\alpha = 0.05$. The *P* value is the result of a comparison between the initial baseline ROM and the final ROM of each of the different groups. Significance at $P < 0.05$.

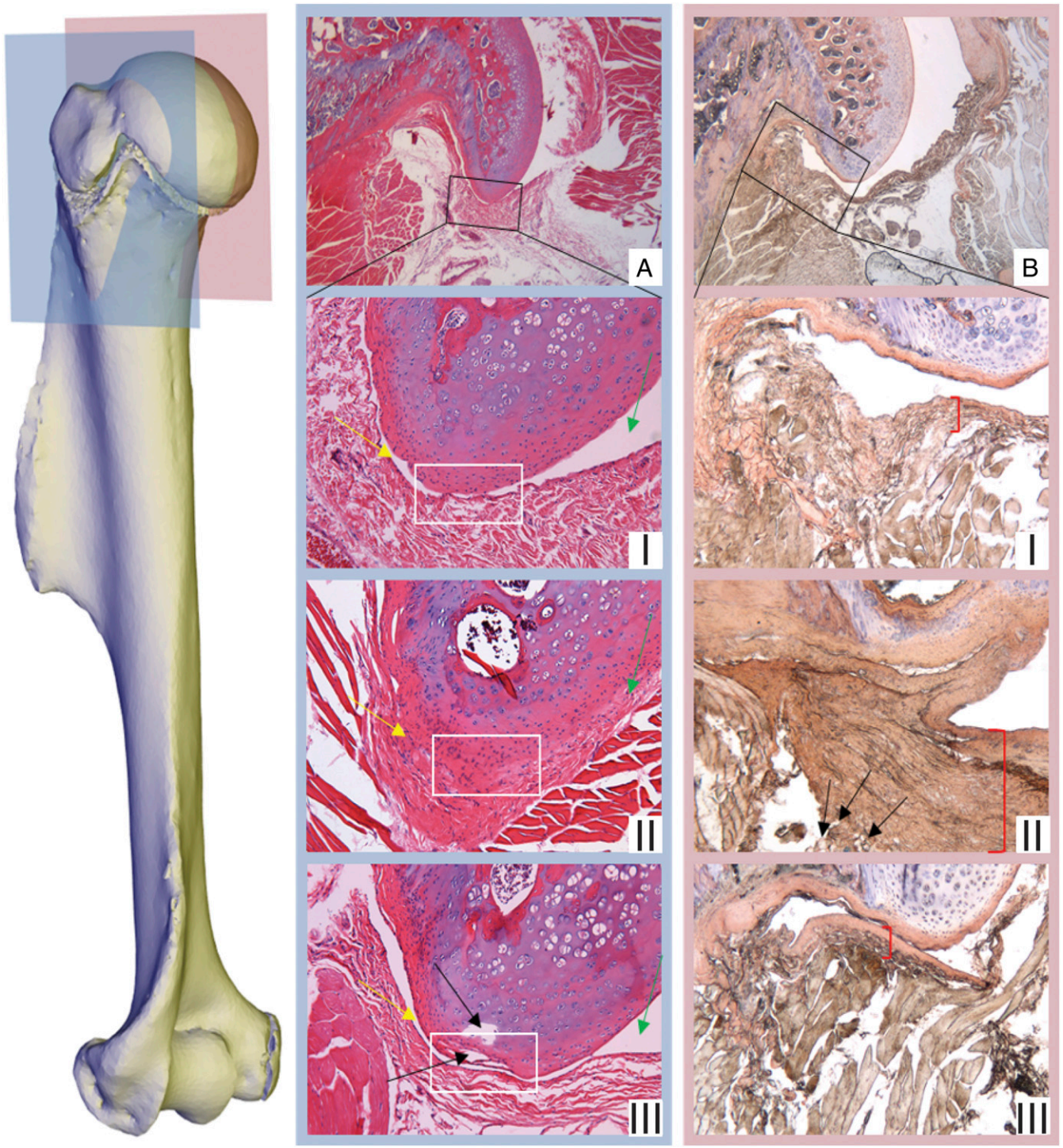

Fig. 4. Coronal histologic sections of the affected humeral head show a reversal of the fibrotic phenotype. Lateral and medial directions correspond to the left and the right of the image, respectively. Colored planes transect the humerus, where the color-coordinated slices were obtained. (*A*) H&E images are taken at 2.5× magnification. Subsequent H&E images are taken at 10× magnification. (*B*) Section stained for fibronectin taken at 2.5× magnification. Subsequent fibronectin images are taken at 5× magnification. (*I*) denotes healthy baseline, (*II*) denotes untreated control, and (*III*) denotes mIA relaxin-2–treated group.

In an established arthrofibrotic contracture model (40, 47, 69), treatment with multiple IA injections of relaxin-2 significantly improves total ROM, returning it to baseline levels measured before limb immobilization. A return to normal ROM is not observed with the sIA and mIV treatment groups, even though the sIA single dose was threefold greater than the single dose of the mIA, and the total mIV treatment dose was 340-fold greater in concentration than that of the total mIA dose. For the sIA treatment group, a temporary and significant improvement in ROM occurs immediately after the single injection (Fig. 3), but its effect is short-lived. This result is consistent with the short in vivo half-life of relaxin-2. By the second measurement, the mIA group received its second dosage of treatment of 2.0 μg/kg, whereas the sIA group received none. This suggests that a sustained,

lower-level dosage is more effective at treatment than a singular large dose (2.0 μg/kg vs. 6 μg/kg), as the rate of improvement by the second measurement was higher in the mIA case. Furthermore, this dose did not lead to seroconversion as titers against human relaxin-2 were not detectable in the rat serum over the course of 8 wk (*SI Appendix*, Fig. S8).

Final torque values in the mIA treatment group also recover to baseline values (Fig. 3*D*), unlike those in the sIA and mIV treatment groups. The similarity between the final ROM and torque values obtained with the mIA treatment group and those measured at baseline demonstrate full recovery of mobility and biomechanical normalcy within the joint after relaxin-2 treatment. When examining external and internal ROM separately, external ROM shows minimal change due to the externally rotated starting position of the rat's forelimb during measurement. As a result, the ROM improvements are predominantly observed during internal rotation. Also, the absence of ROM increases in the contralateral limb indicates that there are no apparent systemic effects on joint laxity from IA application in a distant joint. However, a general trend toward decreased ROM over all groups within their contralateral shoulders may suggest that the immobilization technique in the target shoulder may mildly discourage mobility in the contralateral joint as well (Table 4 and *SI Appendix*, Fig. S6).

The histological hallmarks of contracture are present in the untreated control animals with the presence of fibrotic adhesions and loss of joint space. Fibronectin staining shows thickening of the axillary pouch and adipocyte infiltration. Upon mIA injection of relaxin-2 the fibrotic adhesions are no longer present, there is a lack of adipocyte infiltration, the joint space is clearly defined, and the cellular organization along the capsular surface returns to the normal tangential orientation. Both biomechanically and histologically, arthrofibrosis is reversed to a healthier joint state. Upon closer examination, minor cellular fibrillation is present in the relaxin-2 mIA treatment group sections compared with the healthy baseline. This suggests that an excess of collagen reuptake may have occurred. Thus, an optimized dose, which is likely joint-size-dependent, requires careful titration to achieve the therapeutic goal of restoring joint motion while minimizing off-target effects. The toxicity, pharmacokinetic profile, and adverse side effects of relaxin-2 have been evaluated previously (42). In the abovementioned phase III clinical trial evaluating the use of relaxin-2 for the treatment of acute heart failure, patients safely received a dosage of 30 μg/kg over a 48-h infusion, suggesting that our effective mIA dosing of 10 μg/kg will be well tolerated (42, 43).

Translation of this finding to evaluation in a human clinical trial will require a number of subsequent steps. Although the efficacy study was performed in an established shoulder joint contracture model, its evaluation in a second murine study containing both female and male rats as well as a larger animal model will likely be needed. The former is of interest, because progesterone and high doses of estrogen up-regulate RXFP1, while testosterone down-regulates the same receptor (70–72). As a result, using only female rats is a limitation of this study, as the efficacy of relaxin-2 in females may differ from that in males. However, males also naturally express relaxin-2 and RXFP1 at baseline levels similar to females and show active RXFP1 expression in ligaments, tendons, and joint capsular tissues (51, 73, 74). Relaxin-2 must be prepared under good manufacturing practice for subsequent safety testing as required by a regulatory body. A dosing study will be required to determine the minimally effective relaxin-2 tissue concentrations necessary to reverse the arthrofibrotic phenotype while accounting for other factors that may desensitize the RXFP1 receptor in a human (75). As a potential protein therapeutic for arthrofibrosis, human relaxin-2 joins a substantial list of proteins regulatory-approved, undergoing clinical evaluation, or in preclinical development (76). Relaxin-2 has already been used in clinical studies to assess its antifibrotic potential in scleroderma and for cervical ripening (77–79). Its localized administration may prove to be more efficacious than systemic administration so that it reaches the target tissues at the requisite therapeutic dose before being rapidly cleared or degraded. Although relaxin-2 has shown limited success in translation from rodent models to humans to date (77), its efficacy may be altered and improved by its means of delivery as shown in this work. This in combination with high selectivity, specificity, and in vivo safety inherent to protein therapeutics makes relaxin-2 a strong contender for translation to the clinic (80–82).

In summary, IA injection of relaxin-2 alleviates arthrofibrosis in a murine model of shoulder contracture. Arthrofibrosis is not restricted to the shoulder and is a widespread disease, occurring in all joints after trauma, surgical procedures, prolonged joint immobilization, or from continued daily use. Its high incidence, limited treatment options, and poor patient outcomes call for alternative and effective nonsurgical solutions. Our findings support further development and clinical evaluation of relaxin-2 as a first-in-kind therapy for arthrofibrosis, a condition affecting millions of individuals annually.

Materials and Methods

Detailed description of materials, methods, and associated protocols can be found in *SI Appendix*, along with Western blot and cAMP accumulation analyses, confocal imaging, and pharmacokinetic studies including immuno- and histochemical and relaxin-2 quantitation.

Human Relaxin-2. Recombinant human relaxin-2 was obtained from the Relaxin RRCA Foundation and previously validated by published cAMP accumulation assay and Western blot. Silver-stained SDS/PAGE analysis shows that relaxin-2 is pure (*SI Appendix*, Fig. S1*A*) and MALDI-TOF analysis shows the correct molecular weights of the complete protein as well as its A and B chain constituents (*SI Appendix*, Fig. S1*B*)

Cell Culture Maintenance. Primary HFLS were maintained in complete synoviocyte growth medium (Cell Applications Inc.). HFLS were incubated in a humidified 37 °C incubator with 5% CO_2.

In Vivo Experiments. With the approval of the Institutional Animal Care and Use Committee (IACUC) at Beth Israel Deaconess Medical Center (BIDMC), 20 Female Sprague-Dawley rats (250 to 300 g; Charles River Laboratories, Inc.) were chosen for this study. Baseline ROM measurements were taken for both forelimbs of each rat. Torque measurements were recorded at 100° of internal rotation (τ_{INT}) and 60° of external rotation (τ_{OUT}), totaling a full 160 ° ROM (*SI Appendix*, Figs. S5 and S6). These measurements were required, as they indicate a healthy baseline for normal torque necessary to achieve both rotations. The specific rotation angles were chosen under fluoroscopic guidance to ensure minimal scapular recruitment, while simultaneously allowing for maximum humeral rotation within the joint space. Each ROM measurement was repeated three times to ensure consistency. All measurements were also performed under anesthesia to prevent any active muscle activation from interfering with the passive capsular resistance. Animals were anesthetized with 5% isoflurane inhalation at induction, followed by a 2% isoflurane maintenance dose.

After the baseline measurements and under anesthesia, 20 rats were subjected to the immobilization procedure, as outlined by Villa-Camacho et al. (40), to induce fibrosis. Briefly, an incision was created longitudinally on the left limb, perpendicular to the scapular spine, to expose both the scapula and the humerus. A no. 2-0 Ethibond polyester suture (Ethicon) was used to immobilize the humerus to the scapula by passing two loops through the medial border of the scapula and against the humeral shaft (*SI Appendix*, Figs. S5*A*). Care was taken to ensure the sutures avoided critical vasculature, musculature, and nerves. Each rat was maintained under fixation for 8 wk. At the conclusion of the eighth week, the suture fixations were removed, and the rats were randomly placed in four groups: (*i*) IA relaxin-2, single dose (sIA) ($n = 5$); (*ii*) IA relaxin-2, multiple doses (mIA) ($n = 5$); (*iii*) i.v. relaxin-2, multiple doses (mIV) ($n = 5$); and (*iv*) untreated surgical controls ($n = 5$). The sample size was determined with a power of 0.80 and $\alpha = 0.05$ for a 10% change in ROM from contracted state.

Mechanical Testing Apparatus. The mechanical testing apparatus was assembled with four core components and controlled with a computer through custom-built software written on MATLAB 7.13.0.564 (The MathWorks, Inc.).

Movement of the forelimb was mediated by a stepper motor controlled by a microcontroller (UNO R3; Arduino). The motor was then positioned axially with the reaction torque sensor (TFF400; FUTEK Advanced Sensor Technology, Inc.), which measured torque and was utilized as an input feedback for the system. Along the same axis, the arm clamp and the three-axis inclinometer (3DM-GX3-15; MicroStrain, Inc.) were attached on the sensing side of the torque sensor. The inclinometer also provided both positional feedback as well as angular measurements for the system. The entire assembly was positioned above the rat with the sensing plane parallel to the ground to ensure that gravity had little impact on the torque measurements (*SI Appendix*, Fig. S5). The apparatus was programmed to move to a specified torque or angle for internal and external rotation for each rat. Plastic zip ties were used to secure the rat forelimb in the apparatus. Care was taken to prevent any injury, and the apparatus was programmed with an internal and external limit switch in the case the apparatus operated abnormally.

Treatment and Measurement of Study Groups. Immediately after removal of the restraining sutures, relaxin-2 was administered to the non-control-group rats. There were three different treatment groups: mIA, sIA, and mIV. For the groups requiring IA treatment, human relaxin-2 was administered by IA injection into the anesthetized rats under fluoroscopic guidance and was dosed at 1.50 μg relaxin-2 diluted in 100 μL of PBS (6 μg/kg). For the groups that required multiple doses, IA doses of relaxin-2 were administered every 2 d for 10 d (five relaxin-2 doses of 2 μg/kg for a total dose of 10 μg/kg). Relaxin-2 that was dispensed by i.v. injection through the tail was dosed at 680 μg/kg relaxin-2 diluted in 100 μL PBS. Multiple i.v. tail vain injections were also given every 2 d for 10 d (five relaxin-2 doses of 680 μg/kg for a total dose of 3.4 mg/kg). For days where treatment and ROM measurement overlapped, treatment was administered first. Injection of each IA aliquot of relaxin-2 was performed with a 27-gauge needle (PrecisionGlide; Becton, Dickinson and Company).

Subsequent kinetic measurements were performed randomly and in a blinded manner after treatment. Each measurement was longitudinally spaced in the follow-up period of 8 wk as determined by a previous study (40). These measurements examined the change in ROM angles by using the τ_{INT} and τ_{OUT} recorded at baseline as a reference threshold. The apparatus was programmed so that each rat was measured based on its own individual baseline torque values. This was done to eliminate any variation across rats, allowing each rat to reach an individualized torque that corresponds to their specific baseline ROM (40). Each of these measurements occurred twice per week within the first 2 wk and then weekly throughout the follow-up period. This scheduling was done to limit specimen exposure to isoflurane. Additionally, kinetic changes had been found to occur rapidly only within the first 2 wk and became generally steady for the remainder of the 8 wk (40). Each measurement was taken under anesthesia and repeated three times for both forelimbs to ensure accuracy.

Immunohistologic Analysis. After the follow-up period, the rats were handled according to IACUC guidelines. The rats were weighed and then subjected to CO_2 and bilateral thoracotomy. The shoulders were bilaterally harvested by disarticulating the humerus from the ulna, and removing the scapula from the clavicle and the thoracic cavity. Excess muscle tissue not immediately surrounding the glenohumeral joint capsule was removed. The excised shoulders were decalcified for 2 mo in a solution of EDTA, which was changed four times per week. Once decalcified, the shoulders were affixed in a solution of 10% formalin and then mounted in paraffin stacks for histological sectioning at BIDMC Histology Core. These stacks were mounted so that coronal slicing could be obtained. The slices were stained with H&E and examined for any morphological changes. These slices were taken from a posterior region of the humeral head to better find evidence of periarticular adhesions (83, 84). Further slices, taken midcoronally, were also stained with mouse monoclonal antibody to fibronectin (1:200 concentration; Novus Biologicals) and incubated with peroxidase-conjugated donkey anti-mouse secondary antibody and DAB (3,3-diaminobenzidine) as an enzyme substrate. Harris hematoxylin was used as a counterstain. Collagen III, αSMA, and other acute fibrotic markers were not chosen for analysis, since histologic sectioning would occur 4 mo after contracture creation.

The specimens chosen to undergo histological analysis were the untreated control group and the mIA group. The mIA group was chosen because this group presented with the greatest change in joint ROM in response to therapy and therefore was the best candidate to showcase any morphologic changes due to relaxin-2 administration. The contralateral shoulders from the untreated control group were used to model a healthy control shoulder for histologic comparisons.

Data and Statistical Analysis. Comparisons in kinetic changes were done by comparing the change in ROM between the baseline measurement and the measurements that followed immobilization and treatment. The change in ROM was calculated using a MATLAB script to maintain proper randomization and blinded data processing for the comparisons. ROM measurements were shown as total ROM averages along with 95% CIs. SDs described all variances. Changes in ROM were examined across groups at each measurement time point. Statistical differences across groups were performed by repeated measures ANOVA and Tukey honestly significant difference test. Significance was determined using an alpha level of 0.05 ($P < 0.05$), and CIs of 95% were chosen. Tests for normality were defined using the Shapiro–Wilk test for normality.

ACKNOWLEDGMENTS. We acknowledge Dr. Matthew Warman from the Orthopedic Research Laboratories at Boston Children's Hospital and Harvard Medical School for help with histology and for insightful comments during manuscript preparation. We also thank the Relaxin RRCA Foundation for the gift of recombinant human relaxin-2. Also, we acknowledge Dr. Rosalynn Nazarian (Pathology Service, Massachusetts General Hospital) for reviewing the histology. We acknowledge Mr. and Mrs. Tom and Phyllis Froeschle and the Boston University Ignition Award for providing financial support toward this project.

1. P. S. Vezeridis, D. P. Goel, A. A. Shah, S. Y. Sung, J. J. Warner, Postarthroscopic arthrofibrosis of the shoulder. *Sports Med. Arthrosc. Rev.* **18**, 198–206 (2010).
2. K. E. DeHaven, A. J. Cosgarea, W. J. Sebastianelli, Arthrofibrosis of the knee following ligament surgery. *Instr. Course Lect.* **52**, 369–381 (2003).
3. P. F. Sharkey, W. J. Hozack, R. H. Rothman, S. Shastri, S. M. Jacoby, Insall Award paper. Why are total knee arthroplasties failing today? *Clin. Orthop. Relat. Res.* **2002**, 7–13 (2002).
4. P. J. Papagelopoulos *et al*., Complications after tibia plateau fracture surgery. *Injury* **37**, 475–484 (2006).
5. H. V. Le, S. J. Lee, A. Nazarian, E. K. Rodriguez, Adhesive capsulitis of the shoulder: Review of pathophysiology and current clinical treatments. *Shoulder Elbow* **9**, 75–84 (2017).
6. K. Wong, G. Trudel, O. Laneuville, Noninflammatory joint contractures arising from immobility: Animal models to future treatments. *BioMed Res. Int.* **2015**, 848290 (2015).
7. I. McAlister, S. A. Sems, Arthrofibrosis after periarticular fracture fixation. *Orthop. Clin. North Am.* **47**, 345–355 (2016).
8. M. C. S. Inacio, E. W. Paxton, S. E. Graves, R. S. Namba, S. Nemes, Projected increase in total knee arthroplasty in the United States–An alternative projection model. *Osteoarthritis Cartilage* **25**, 1797–1803 (2017).
9. B. M. Bodendorfer *et al*., Outcomes and predictors of success for arthroscopic lysis of adhesions for the stiff total knee arthroplasty. *Orthopedics* **40**, e1062–e1068 (2017).
10. N. S. Kalson *et al*., International consensus on the definition and classification of fibrosis of the knee joint. *Bone Joint J.* **98-B**, 1479–1488 (2016).
11. T. L. Sanders *et al*., Incidence of and factors associated with the decision to undergo anterior cruciate ligament reconstruction 1 to 10 Years after injury. *Am. J. Sports Med.* **44**, 1558–1564 (2016).
12. T. L. Sanders *et al*., Procedural intervention for arthrofibrosis after ACL reconstruction: Trends over two decades. *Knee Surg. Sports Traumatol. Arthrosc.* **25**, 532–537 (2017).
13. S. Ekhtiari *et al*., Arthrofibrosis after ACL reconstruction is best treated in a step-wise approach with early recognition and intervention: A systematic review. *Knee Surg. Sports Traumatol. Arthrosc.* **25**, 3929–3937 (2017).
14. S. Kim, J. Bosque, J. P. Meehan, A. Jamali, R. Marder, Increase in outpatient knee arthroscopy in the United States: A comparison of National Surveys of Ambulatory Surgery, 1996 and 2006. *J. Bone Joint Surg. Am.* **93**, 994–1000 (2011).
15. K. S. Austin, O. H. Sherman, Complications of arthroscopic meniscal repair. *Am. J. Sports Med.* **21**, 864–868, discussion 868–869 (1993).
16. S. Amin, S. J. Achenbach, E. J. Atkinson, S. Khosla, L. J. Melton, 3rd, Trends in fracture incidence: A population-based study over 20 years. *J. Bone Miner. Res.* **29**, 581–589 (2014).
17. R. Mittal, Posttraumatic stiff elbow. *Indian J. Orthop.* **51**, 4–13 (2017).
18. S. H. Kim, R. M. Szabo, R. A. Marder, Epidemiology of humerus fractures in the United States: Nationwide emergency department sample, 2008. *Arthritis Care Res. (Hoboken)* **64**, 407–414 (2012).
19. B. van Loghum, Functional outcomes for unstable distal radial fractures treated with open reduction and internal fixation or closed reduction and percutaneous fixation. A propsective randomized trial. *Ned tijdsschrift voor Traumachirurgie* **1**, 24–25 (2010).
20. L. B. Kempton, M. Balasubramaniam, E. Ankerson, J. M. Wiater, A radiographic analysis of the effects of prosthesis design on scapular notching following reverse total shoulder arthroplasty. *J. Shoulder Elbow Surg.* **20**, 571–576 (2011).
21. D. Gittings *et al*., Arthroscopic lysis of adhesions improves knee range of motion after fixation of intra-articular fractures about the knee. *Arch. Orthop. Trauma Surg.* **136**, 1631–1635 (2016).
22. M. T. Nagy, R. J. Macfarlane, Y. Khan, M. Waseem, The frozen shoulder: Myths and realities. *Open Orthop. J.* **7**, 352–355 (2013).
23. J. P. Wang *et al*., Manipulation under anaesthesia for frozen shoulder in patients with and without non-insulin dependent diabetes mellitus. *Int. Orthop.* **34**, 1227–1232 (2010).

24. J. E. Hsu, O. A. Anakwenze, W. J. Warrender, J. A. Abboud, Current review of adhesive capsulitis. *J. Shoulder Elbow Surg.* **20**, 502–514 (2011).
25. A. I. Binder, D. Y. Bulgen, B. L. Hazleman, S. Roberts, Frozen shoulder: A long-term prospective study. *Ann. Rheum. Dis.* **43**, 361–364 (1984).
26. A. S. Neviaser, J. A. Hannafin, Adhesive capsulitis: A review of current treatment. *Am. J. Sports Med.* **38**, 2346–2356 (2010).
27. C. S. Samuel, E. D. Lekgabe, I. Mookerjee, (2007) "The effects of relaxin on extracellular matrix remodeling in health and fibrotic disease" in *Relaxin and Related Peptides*, A. Agoulnik, Ed. (Springer, New York), pp. 88–103.
28. C. S. Samuel *et al*., Relaxin modulates cardiac fibroblast proliferation, differentiation, and collagen production and reverses cardiac fibrosis in vivo. *Endocrinology* **145**, 4125–4133 (2004).
29. G. A. McDonald *et al*., Relaxin increases ubiquitin-dependent degradation of fibronectin in vitro and ameliorates renal fibrosis in vivo. *Am. J. Physiol. Renal. Physiol.* **285**, F59–F67 (2003).
30. J. Grossman, W. H. Frishman, Relaxin: A new approach for the treatment of acute congestive heart failure. *Cardiol. Rev.* **18**, 305–312 (2010).
31. J. M. Sasser, New targets for renal interstitial fibrosis: Relaxin family peptide receptor 1-angiotensin type 2 receptor heterodimers. *Kidney Int.* **86**, 9–10 (2014).
32. J. R. Teerlink *et al*., Serelaxin in addition to standard therapy in acute heart failure: Rationale and design of the RELAX-AHF-2 study. *Eur. J. Heart Fail.* **19**, 800–809 (2017).
33. R. G. Bennett, Relaxin and its role in the development and treatment of fibrosis. *Transl. Res.* **154**, 1–6 (2009).
34. D. Bani, M. Bigazzi, Relaxin as a cardiovascular drug: A promise kept. *Curr. Drug Saf.* **6**, 324–328 (2011).
35. A. Pini *et al*., Protection from cigarette smoke-induced vascular injury by recombinant human relaxin-2 (serelaxin). *J. Cell. Mol. Med.* **20**, 891–902 (2016).
36. K. Ohtera *et al*., Effect of pregnancy on joint contracture in the rat knee. *J. Appl. Physiol.* **92**, 1494–1498 (2002).
37. A. Jeyabalan *et al*., Matrix metalloproteinase-2 activity, protein, mRNA, and tissue inhibitors in small arteries from pregnant and relaxin-treated nonpregnant rats. *J. Appl. Physiol.* **100**, 1955–1963 (2006).
38. G. Trudel, H. K. Uhthoff, Contractures secondary to immobility: Is the restriction articular or muscular? An experimental longitudinal study in the rat knee. *Arch. Phys. Med. Rehabil.* **81**, 6–13 (2000).
39. D. Bani *et al*., A novel, simple bioactivity assay for relaxin based on inhibition of platelet aggregation. *Regul. Pept.* **144**, 10–16 (2007).
40. J. C. Villa-Camacho *et al*., In vivo kinetic evaluation of an adhesive capsulitis model in rats. *J. Shoulder Elbow Surg.* **24**, 1809–1816 (2015).
41. P. A. Cossum *et al*., The disposition of a human relaxin (hRlx-2) in pregnant and nonpregnant rats. *Pharm. Res.* **9**, 419–424 (1992).
42. S. S. Wilson, S. I. Ayaz, P. D. Levy, Relaxin: A novel agent for the treatment of acute heart failure. *Pharmacotherapy* **35**, 315–327 (2015).
43. L. DeFrancesco, Drug pipeline 3Q13. *Nat. Biotechnol.* **31**, 956 (2013).
44. K. H. Lee *et al*., Adhesive capsulitis of the shoulder joint: Value of glenohumeral distance on magnetic resonance arthrography. *J. Comput. Assist. Tomogr.* **41**, 116–120 (2017).
45. S. S. Glasson, M. G. Chambers, W. B. Van Den Berg, C. B. Little, The OARSI histopathology initiative–Recommendations for histological assessments of osteoarthritis in the mouse. *Osteoarthritis Cartilage* **18** (suppl. 3), S17–S23 (2010).
46. K. P. Pritzker *et al*., Osteoarthritis cartilage histopathology: Grading and staging. *Osteoarthritis Cartilage* **14**, 13–29 (2006).
47. D. H. Kim *et al*., Characterization of a frozen shoulder model using immobilization in rats. *J. Orthop. Surg. Res.* **11**, 160 (2016).
48. B. A. Goldberg, M. M. Scarlat, D. T. Harryman, 2nd, Management of the stiff shoulder. *J. Orthop. Sci.* **4**, 462–471 (1999).
49. S. L. Teichman *et al*., Relaxin, a pleiotropic vasodilator for the treatment of heart failure. *Heart Fail. Rev.* **14**, 321–329 (2009).
50. V. Cernaro *et al*., Relaxin: New pathophysiological aspects and pharmacological perspectives for an old protein. *Med. Res. Rev.* **34**, 77–105 (2014).
51. J. H. Kim, S. K. Lee, S. K. Lee, J. H. Kim, M. Fredericson, Relaxin receptor RXFP1 and RXFP2 expression in ligament, tendon, and shoulder joint capsule of rats. *J. Korean Med. Sci.* **31**, 983–988 (2016).
52. D. J. Scott *et al*., Identification and characterization of the mouse and rat relaxin receptors as the novel orthologues of human leucine-rich repeat-containing G-protein-coupled receptor 7. *Clin. Exp. Pharmacol. Physiol.* **31**, 828–832 (2004).
53. B. L. Ferraiolo, J. Winslow, G. Laramee, A. Celniker, P. Johnston, The pharmacokinetics and metabolism of human relaxins in rhesus monkeys. *Pharm. Res.* **8**, 1032–1038 (1991).
54. M. Dahlke *et al*., Safety and tolerability of serelaxin, a recombinant human relaxin-2 in development for the treatment of acute heart failure, in healthy Japanese volunteers and a comparison of pharmacokinetics and pharmacodynamics in healthy Japanese and Caucasian populations. *J. Clin. Pharmacol.* **55**, 415–422 (2015).
55. C. S. Samuel, Relaxin: Antifibrotic properties and effects in models of disease. *Clin. Med. Res.* **3**, 241–249 (2005).
56. T. D. Bunker, Time for a new name for 'frozen shoulder'. *Br. Med. J. (Clin. Res. Ed.)* **290**, 1233–1234 (1985).
57. T. D. Bunker, J. Reilly, K. S. Baird, D. L. Hamblen, Expression of growth factors, cytokines and matrix metalloproteinases in frozen shoulder. *J. Bone Joint Surg. Br.* **82**, 768–773 (2000).
58. C. Sassoli *et al*., Relaxin prevents cardiac fibroblast-myofibroblast transition via notch-1-mediated inhibition of TGF-β/Smad3 signaling. *PLoS One* **8**, e63896 (2013).
59. C. Wang *et al*., The anti-fibrotic actions of relaxin are mediated through a NO-sGC-cGMP-dependent pathway in renal myofibroblasts in vitro and enhanced by the NO donor, diethylamine NONOate. *Front. Pharmacol.* **7**, 91 (2016).
60. A. Desmoulière, A. Geinoz, F. Gabbiani, G. Gabbiani, Transforming growth factor-beta 1 induces alpha-smooth muscle actin expression in granulation tissue myofibroblasts and in quiescent and growing cultured fibroblasts. *J. Cell Biol.* **122**, 103–111 (1993).
61. R. S. Watson *et al*., Gene delivery of TGF-β1 induces arthrofibrosis and chondrometaplasia of synovium in vivo. *Lab. Invest.* **90**, 1615–1627 (2010).
62. F. N. Unterhauser, U. Bosch, J. Zeichen, A. Weiler, Alpha-smooth muscle actin containing contractile fibroblastic cells in human knee arthrofibrosis tissue. Winner of the AGA-DonJoy Award 2003. *Arch. Orthop. Trauma Surg.* **124**, 585–591 (2004).
63. C. S. Samuel, J. P. Coghlan, J. F. Bateman, Effects of relaxin, pregnancy and parturition on collagen metabolism in the rat pubic symphysis. *J. Endocrinol.* **159**, 117–125 (1998).
64. L. T. Goldsmith, G. Weiss, B. G. Steinetz, Relaxin and its role in pregnancy. *Endocrinol. Metab. Clin. North Am.* **24**, 171–186 (1995).
65. C. W. Schauberger *et al*., Peripheral joint laxity increases in pregnancy but does not correlate with serum relaxin levels. *Am. J. Obstet. Gynecol.* **174**, 667–671 (1996).
66. S. C. Kwok, D. Chakraborty, M. J. Soares, G. Dai, Relative expression of proprotein convertases in rat ovaries during pregnancy. *J. Ovarian Res.* **6**, 91 (2013).
67. O. D. Sherwood, V. E. Crnekovic, Development of a homologous radioimmunoassay for rat relaxin. *Endocrinology* **104**, 893–897 (1979).
68. O. D. Sherwood, V. E. Crnekovic, W. L. Gordon, J. E. Rutherford, Radioimmunoassay of relaxin throughout pregnancy and during parturition in the rat. *Endocrinology* **107**, 691–698 (1980).
69. A. Kanno, H. Sano, E. Itoi, Development of a shoulder contracture model in rats. *J. Shoulder Elbow Surg.* **19**, 700–708 (2010).
70. F. Dehghan, S. Muniandy, A. Yusof, N. Salleh, Testosterone reduces knee passive range of motion and expression of relaxin receptor isoforms via 5α-dihydrotestosterone and androgen receptor binding. *Int. J. Mol. Sci.* **15**, 4619–4634 (2014).
71. D. A. Faryniarz, M. Bhargava, C. Lajam, E. T. Attia, J. A. Hannafin, Quantitation of estrogen receptors and relaxin binding in human anterior cruciate ligament fibroblasts. *In Vitro Cell. Dev. Biol. Anim.* **42**, 176–181 (2006).
72. F. Dehghan *et al*., Changes in knee laxity and relaxin receptor isoforms expression (RXFP1/RXFP2) in the knee throughout estrous cycle phases in rodents. *PLoS One* **11**, e0160984 (2016).
73. A. I. Agoulnik, Relaxin and related peptides in male reproduction. *Adv. Exp. Med. Biol.* **612**, 49–64 (2007).
74. J. M. Wolf, K. L. Cameron, K. B. Clifton, B. D. Owens, Serum relaxin levels in young athletic men are comparable with those in women. *Orthopedics* **36**, 128–131 (2013).
75. A. Kern, G. D. Bryant-Greenwood, Characterization of relaxin receptor (RXFP1) desensitization and internalization in primary human decidual cells and RXFP1-transfected HEK293 cells. *Endocrinology* **150**, 2419–2428 (2009).
76. K. Jayapal, K. Wlaschin, W. Hu, M. G. S. Yap, Recombinant protein therapeutics from CHO cells-20 years and counting. *Chem. Eng. Prog.* **103**, 40 (2007).
77. E. Unemori, Serelaxin in clinical development: Past, present and future. *Br. J. Pharmacol.* **174**, 921–932 (2017).
78. D. Khanna *et al*.; Relaxin Investigators and the Scleroderma Clinical Trials Consortium Recombinant human relaxin in the treatment of systemic sclerosis with diffuse cutaneous involvement: A randomized, double-blind, placebo-controlled trial. *Arthritis Rheum.* **60**, 1102–1111 (2009).
79. G. Weiss *et al*., Recombinant human relaxin versus placebo for cervical ripening: A double-blind randomised trial in pregnant women scheduled for induction of labour. *BMC Pregnancy Childbirth* **16**, 260 (2016).
80. S. D. Putney, P. A. Burke, Improving protein therapeutics with sustained-release formulations. *Nat. Biotechnol.* **16**, 153–157 (1998).
81. S. Mitragotri, P. A. Burke, R. Langer, Overcoming the challenges in administering biopharmaceuticals: Formulation and delivery strategies. *Nat. Rev. Drug Discov.* **13**, 655–672 (2014).
82. B. Leader, Q. J. Baca, D. E. Golan, Protein therapeutics: A summary and pharmacological classification. *Nat. Rev. Drug Discov.* **7**, 21–39 (2008).
83. Y. Zhang, M. Huo, J. Zhou, S. Xie, PKSolver: An add-in program for pharmacokinetic and pharmacodynamic data analysis in Microsoft Excel. *Comput. Methods Programs Biomed.* **99**, 306–314 (2010).
84. S. Brue *et al*., Idiopathic adhesive capsulitis of the shoulder: A review. *Knee Surg. Sports Traumatol. Arthrosc.* **15**, 1048–1054 (2007).